

## Supporting Information

### Facile electrospinning formation of carbon-confined metal oxide cube-in-tube nanostructures for stable lithium storage

Ziang Liu,<sup>a†</sup> Ruiting Guo,<sup>a†</sup> Jiashen Meng,<sup>a</sup> Xiong Liu,<sup>a</sup> Xuanpeng Wang,<sup>a</sup> Qi Li<sup>\*a</sup> and Liqiang Mai<sup>\*ab</sup>

<sup>a</sup>State Key Laboratory of Advanced Technology for Materials Synthesis and Processing Wuhan, 430070 Hubei, China

<sup>b</sup>Department of Chemistry, University of California, Berkeley, California 94720, United States.  
E-mail: qi.li@whut.edu.cn, [mlq518@whut.edu.cn](mailto:mlq518@whut.edu.cn);

## Experimental

### Preparation of CoSn(OH)<sub>6</sub> hollow nanocubes

1.40 g tin chloride pentahydrate (SnCl<sub>4</sub>•5H<sub>2</sub>O) was added to 20 mL H<sub>2</sub>O and stirred at room temperature until getting a homogeneous solution (noted as A solution). 0.95 g cobalt chloride hexahydrate (CoCl<sub>2</sub>•6H<sub>2</sub>O) and 1.18 g sodium citrate dihydrate (C<sub>6</sub>H<sub>5</sub>Na<sub>3</sub>O<sub>7</sub>•2H<sub>2</sub>O) were added to 120 mL H<sub>2</sub>O and stirred at room temperature until getting a homogeneous solution (noted as B solution). 1.60 g sodium hydroxide (NaOH) was added to 20 mL H<sub>2</sub>O, stirring and getting a homogeneous solution (noted as C solution). A solution was added into B solution drop by drop, forming a light pink turbid liquid; then C solution was added followed by stirring for 2 h. At last, pink CoSn(OH)<sub>6</sub> powder was obtained after washing and drying in vacuum at 60 °C for 12 h.

### Preparation of CoSnO<sub>3</sub> cube-in-tube nanostructures

First, the precursor solution for electrospinning was prepared with low-molecular-weight (98-99% hydrolyzed), middle-molecular-weight (86-89% hydrolyzed) and high-molecular-weight (98-99% hydrolyzed) polyvinyl alcohol (PVA) in a molar ratio of 3:2:1 (9.5 wt.%) in 20 mL of deionized water. Second, 0.70 g CoSn(OH)<sub>6</sub> powder and 1.80 g manganese acetate tetrahydrate (C<sub>4</sub>H<sub>6</sub>MnO<sub>4</sub>•4H<sub>2</sub>O) were added and stirred at room temperature until getting a uniform turbid solution. Third, the above mix solution was subsequently electrospun at a constant flow rate and at a high voltage of 12 kV (electrospinning equipment: SS-2534H from

UCALERY Co., Beijing, China). The composite nanowires were collected on revolving aluminum foil. Fourth, after drying at 70 °C for 12 h, the composite nanowires were pre-sintered at 300 °C (2 °C/min) in air for 1 h; then annealed at 450 °C (5 °C min<sup>-1</sup>) under the argon atmosphere for 1 h. Finally, uniform hollow cube-in-tube nanostructures were obtained.

### **Characterization**

The crystallographic information of the final products was measured using a Bruker D8 Discover X-ray diffractometer (XRD) equipped with a Cu-K $\alpha$  radiation source; the samples were scanned over a 2 $\theta$  range from 10° to 80° at room temperature. Scanning electron microscope (SEM) images were collected using a JEOL-7100F SEM. Transmission electron microscope (TEM) and high-resolution TEM (HRTEM) images were collected using a JEM-2100F TEM. The Brunauer-Emmett-Teller (BET) specific surface area was calculated from nitrogen adsorption isotherms measured at 77 K using a Tristar-3020 instrument. Energy-dispersive X-ray spectra (EDS) were recorded using an Oxford IE250 system. X-ray photoelectron spectroscopy (XPS) measurements were performed using a VG MultiLab 2000 instrument. Thermogravimetric analysis (TGA) was performed using an STA 449 C. Inductively coupled plasma atomic emission spectrometry (ICP-AES) was performed using a Optima 4300DV.

Type 2016 coin cells were assembled in a glovebox filled with pure argon gas. Lithium foil was used as the counter electrode and a solution of LiPF<sub>6</sub> (1 M) in EC/DEC (1:1 vol/vol) was used as the electrolyte. The anode was composed of a ground mixture of 70 wt.% active material, 20 wt.% acetylene black and 10 wt.% polytetrafluoroethylene. Galvanostatic charge/discharge measurements were performed using a multichannel battery testing system (LAND CT2001A). Cyclic voltammograms (CV) and electrochemical impedance spectra (EIS) were collected using an Autolab potentiostat/galvanostat. Capacities were calculated without binder and conductive additives.

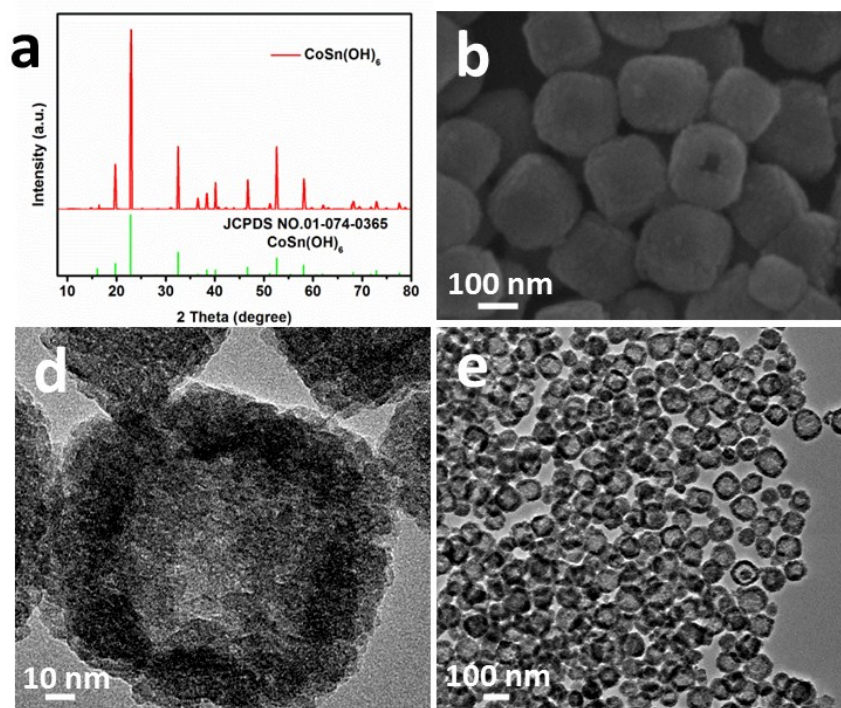


**Fig. S1** (a) XRD pattern, (b) SEM and (c, d) TEM images of pre-prepared  $\text{CoSn}(\text{OH})_6$  nanocubes, respectively.

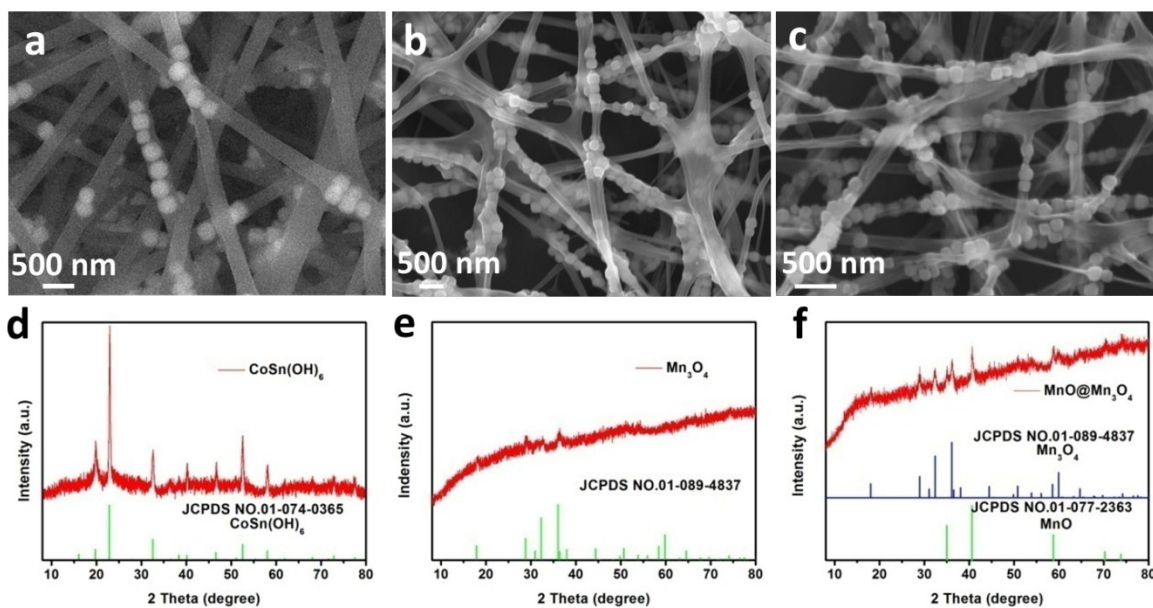


**Fig. S2** SEM images of (a) the as-prepared electrospinning nanofibers, (b) the intermediate product after being heated to  $350\text{ }^\circ\text{C}$  and then held at this temperature for 1 h in air and (c) cube-in-tube nanostructures after being heated to  $450\text{ }^\circ\text{C}$  and held for 1 h in argon atmosphere. (d-f) The corresponding XRD patterns of (a), (b) and (c), respectively.

**Tab. S1** ICP results of the as-prepared cube-in-tube nanostructures.

	Gauged molar concentration (mmol L <sup>-1</sup> )	Gauged Mn/Co (up) Mn/Sn (down)	Theoretical molar concentration (mol L <sup>-1</sup> )	Theoretical Mn/Co (up) Mn/Sn (down)
Co	0.256	3.000	2.503	2.934
Sn	0.260		2.503	
Mn	0.768	2.954	7.344	2.934

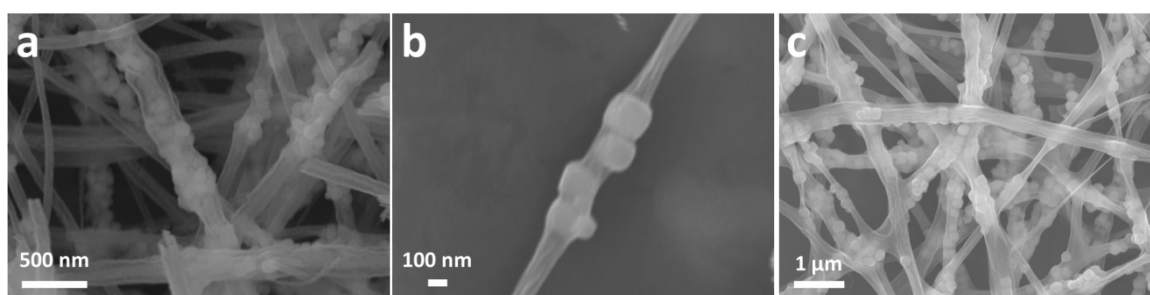


**Fig. S3** SEM images of cube-in-tube nanostructure with different sized nanocubes. (a) SEM image that shows diameter of nanotubes is much larger than that of nanocubes. (b) SEM image that shows diameter of nanotubes is much smaller than that of nanocubes. (c) SEM image that shows diameter of nanotubes matches with nanocubes.

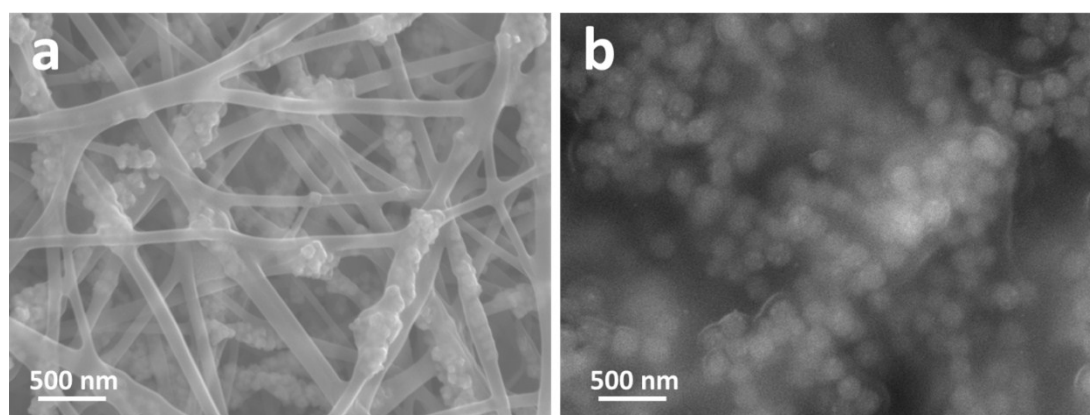


**Fig. S4** SEM images of electrospinning fibers without manganese acetate (a) before sintering and (b) after sintering

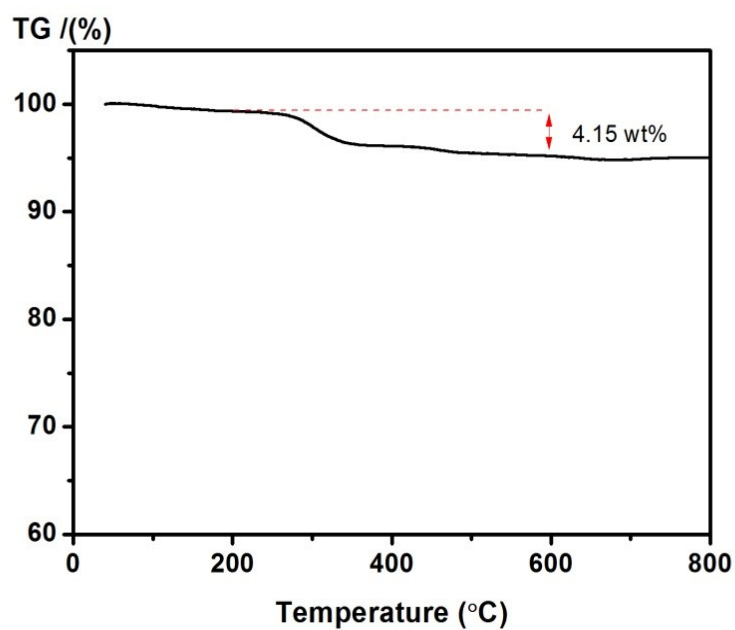


**Fig. S5** TGA curve of the cube-in-tube nanostructures under the air atmosphere at a heating rate of  $10\text{ }^{\circ}\text{C min}^{-1}$ .

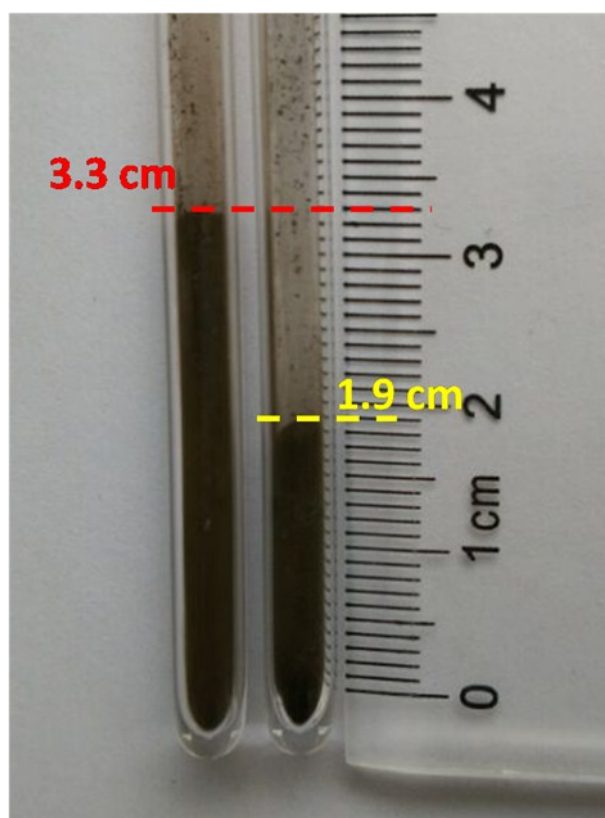


**Fig. S6** Digital photo showing 250 mg of carbon-confined manganese oxide hollow nanotubes (left) and hollow cube-in-tube nanostructures (right) samples which are sufficiently ground and packed under the same condition in quartz tubes with an inner diameter of 6 mm.

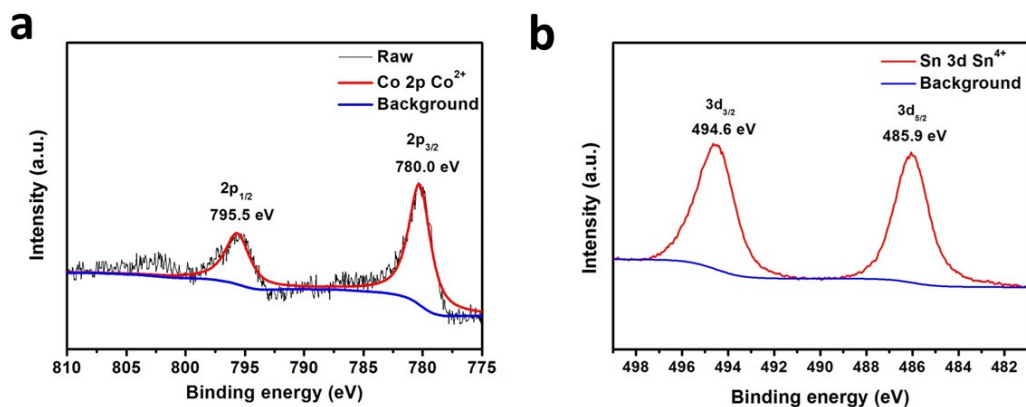


**Fig. S7** (a) Co 2p and Sn 3d XPS spectra of the cube-in-tube nanostructures containing amorphous CoSnO<sub>3</sub>, manganese oxides and carbon.

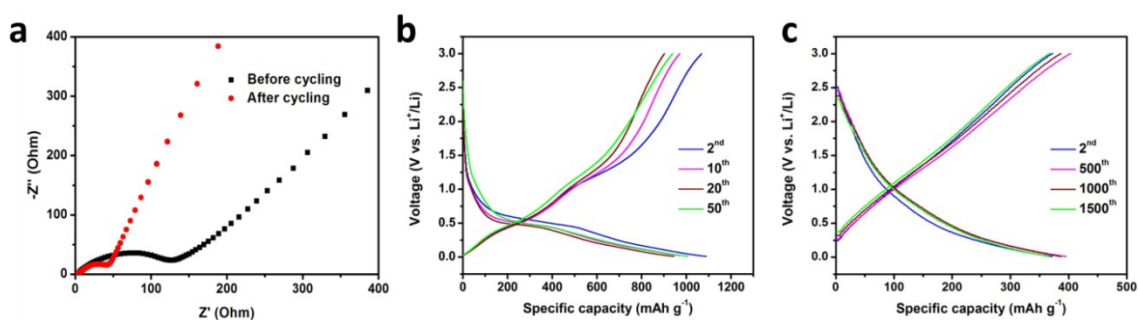


**Fig. S8** (a) AC impedance plots before and after 20 cycles at 3 V (vs Li<sup>+</sup>/Li) and (b) the discharge/charge curves at 0.1 A g<sup>-1</sup> and (c) 2 A g<sup>-1</sup> of the cube-in-tube nanostructures containing amorphous CoSnO<sub>3</sub>, manganese oxides and carbon.

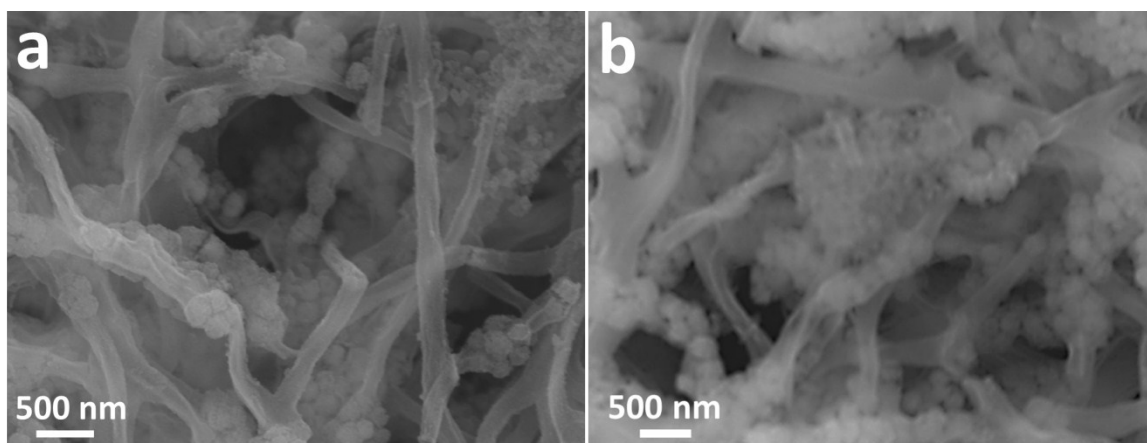


**Fig. S9** SEM images of hollow cube-in-tube nanostructures after rate cycling without removing binder and conductive additives.

**Tab. S2** Electrochemical performance comparison of the cube-in-tube nanostructures (this work) with other anode materials of similar components or structures.

Morphologies	Voltage range (V)	Current densities (mA g <sup>-1</sup> )	Cycle numbers	Residual capacity (mAh g <sup>-1</sup> )	Capacity retention (compare to second cycle)	Reference
CoSnO <sub>3</sub> @MnOx/C	0.01-3	100	65	1173.9	96.55%	Our work
hollow cube-in-tube		2000	1500	367.5	98.95%	
Amorphous CoSnO <sub>3</sub> @C	0.01-1.5	200	400	450	84.91%	S1
CoSnO <sub>3</sub> nanobox/GN/CNTs	0-3	100	150	1098.7	80.60%	S2
CoO-in-CoSnO <sub>3</sub> @C nanotube	0.005-2.5	400	150	695.7	70.10%	S3
CoSnO <sub>3</sub> /Graphene	0.005-3	200	50	724	87.23%	S4
		400		649	79.15%	
MnO@CNFs (MnO 34.6 wt%)	0.01-3	100	150	987	94.00%	S5
		500	280	655	90.97%	
MnO/CNF	0.01-2.5	200	200	398	83.89%	S6
CNF/Mn <sub>3</sub> O <sub>4</sub>	0.02-3	100	50	748	78.30%	S7

- S1. Z. Wang, Z. Wang, W. Liu, W. Xiao and X. W. Lou, *Energy Environ. Sci.*, 2013, **6**, 87-91.
- S2. X. Zhao, G. Wang, Y. Zhou and H. Wang, *Energy*, 2017, **118**, 172-180.
- S3. C. Guan, X. Li, H. Yu, L. Mao, L. H. Wong, Q. Yan and J. Wang, *Nanoscale*, 2014, **6**, 13824-13830.
- S4. Y. Cao, L. Zhang, D. Tao, D. Huo and K. Su, *Electrochim. Acta*, 2014, **132**, 483-489.
- S5. X. Zhao, Y. Du, L. Jin, Y. Yang, S. Wu, W. Li, Y. Yu, Y. Zhu and Q. Zhang, *Sci. Rep.*, 2015, **5**.
- S6. J.-G. Wang, Y. Yang, Z.-H. Huang and F. Kang, *Electrochim. Acta*, 2015, **170**, 164-170.
- S7. S.-H. Park and W.-J. Lee, *J. Power Sources*, 2015, **281**, 301-309.